I&EC research
Industrial & Engineering Chemistry Research

Article

Cite This: Ind. Eng. Chem. Res. 2018, 57, 12736−12741

pubs.acs.org/IECR

Morphology-Dependent Catalytic Performance of NbO_x/CeO_2 Catalysts for Selective Catalytic Reduction of NO_x with NH_3

Zhihua Lian,[†] Wenpo Shan,[†] Yan Zhang,[†] Meng Wang,[†] and Hong He*[,†,‡,§]

[†]Center for Excellence in Regional Atmospheric Environment and Key Laboratory of Urban Pollutant Conversion, Institute of Urban Environment, Chinese Academy of Sciences, Xiamen 361021, China

[‡]State Key Joint Laboratory of Environment Simulation and Pollution Control, Research Center for Eco-Environmental Sciences, Chinese Academy of Sciences, Beijing 100085, China

[§]University of Chinese Academy of Sciences, Beijing 100049, China

ABSTRACT: Nb/CeO_2 catalysts with different morphologies for the selective catalytic reduction of NO_x with NH_3 (NH_3-SCR) were fully studied. A Nb/CeO_2 nanoparticle catalyst presented better NH_3-SCR performance than Nb/CeO_2 nanorods, and a Nb/CeO_2 nanocube catalyst presented the lowest NO_x conversion. Transmission electron microscopy, N_2 physisorption, X-ray powder diffraction, X-ray photoelectron spectroscopy, temperature-programmed reduction with H_2 (H_2-TPR), and diffuse reflectance infrared Fourier transform spectroscopy (DRIFTS) were used to characterize the samples. The obtained results reveal that larger specific surface area, more abundant surface oxygen species and acid sites, lower crystallinity, and stronger redox capability of the Nb/CeO_2 nanoparticle catalyst all contributed to its better NH_3-SCR performance.

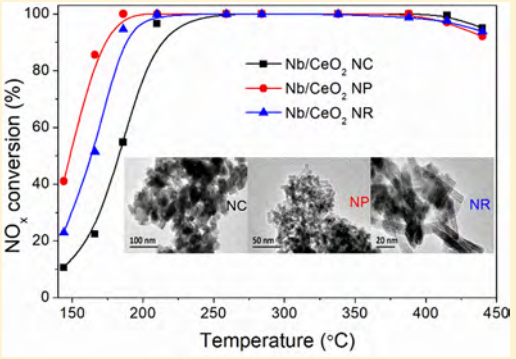

1. INTRODUCTION

Anthropogenic activities, such as the combustion of fossil fuels, emit large quantities of nitrogen oxides (NO_x), which contribute to a number of severe environmental problems, such as ozone depletion, photochemical smog, haze, and acid rain.[1,2] To reduce the emission of NO_x, stringent environmental legislation has been enacted around the world. Selective catalytic reduction of NO_x with NH_3 (NH_3-SCR) is an economical and efficient method to remove NO_x, and V_2O_5-$WO_3(MoO_3)/TiO_2$ catalysts have been widely used.[3−5] However, several inevitable drawbacks of vanadia-based catalysts still remain, for example, their narrow operating temperature window, the toxicity of V_2O_5 toward the environment and human health, and their high oxidation activity toward sulfur dioxide at high temperature.[6−8] Thus, development of efficient and novel catalysts is urgently desired.

CeO_2-based catalysts have been investigated extensively for the NH_3-SCR reaction and show excellent catalytic performance in the medium- or high-temperature ranges as a result of excellent redox properties and high oxygen storage capacity. In our previous study, Ce/TiO_2 and V_2O_5/CeO_2 catalysts exhibited excellent NH_3-SCR activity.[9−11] A number of catalysts supported on CeO_2, such as WO_3/CeO_2 catalysts[12,13] and phosphotungstic acid-modified CeO_2 catalysts (P-W/CeO_2),[14,15] were prepared for NH_3-SCR and presented high NO_x conversion.

The morphology of the catalysts has been found to influence their properties and catalytic activity. Nanosized CeO_2 particles, cubes, and rods were investigated, and CeO_2 nanorods showed the highest catalytic oxidation activity for *o*-xylene.[16] $Pt/BaO/CeO_2$ catalysts, using CeO_2 nanorods, nanocubes, and nanoparticles as supports, were studied for NO_x storage/reduction, and the catalytic activity ranked by the CeO_2 support morphology was nanocubes < nanoparticles < nanorods.[17] The influence of morphology on the activity of $deNO_x$ catalysts has also attracted great interest.[18−22] TiO_2 nanospindles and nanosheets were applied to dispersed vanadia species, and the catalyst dispersed on TiO_2 nanosheets exhibited better NH_3-SCR activity.[18] Compared to the TiO_2 nanoparticle-supported catalyst, the TiO_2 nanosheet-supported $Zr\text{-}CeVO_4$ catalyst showed higher activity, H_2O/SO_2 durability, and stability.[19]

Niobium-based materials have attracted a lot of interest for various reactions, acting as solid acid catalysts, catalyst supports, or catalyst promoters.[23] In our previous studies, the acidity of MnO_x was significantly improved by the introduction of Nb, and $Mn_2Nb_1O_x$ exhibited excellent NO_x conversion and N_2 selectivity.[24] Nb addition was also found to remarkably promote the SCR activity of Ce-based catalysts.[25−28]

In this study, Nb/CeO_2 catalysts derived from CeO_2 nanorods, nanocubes, and nanoparticles for the NH_3-SCR reaction were synthesized by an impregnation route. Among the three shapes of CeO_2, Nb/CeO_2 nanoparticles exhibited the highest NO_x conversion.

Received: June 7, 2018
Revised: August 27, 2018
Accepted: September 4, 2018
Published: September 4, 2018

DOI: 10.1021/acs.iecr.8b02553
Ind. Eng. Chem. Res. 2018, 57, 12736−12741

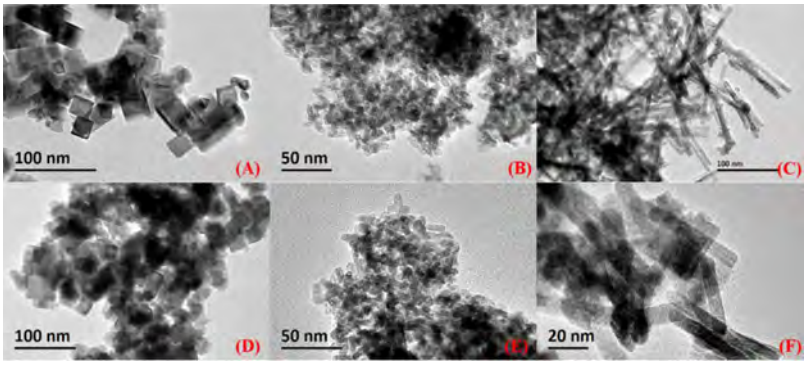

Figure 1. TEM images of (A) CeO_2 NC, (B) CeO_2 NP, (C) CeO_2 NR, (D) Nb/CeO_2 NC, (E), Nb/CeO_2 NP, and (F) Nb/CeO_2 NR.

2. EXPERIMENTAL SECTION

2.1. Synthesis of Catalysts. CeO_2 nanorods (NR), nanoparticles (NP), and nanocubes (NC) were synthesized by a hydrothermal route under different conditions. Deionized water was used to dissolve $Ce(NO_3)_3{\cdot}6H_2O$ and NaOH separately. After the solutions were mixed well, the slurry was heated at 120 °C for 12 h in a Teflon-lined stainless-steel autoclave to produce nanorods (this process was conducted at 200 °C for 24 h for nanocubes and at 30 °C for 12 h for nanoparticles). To remove any possible ionic remnants, deionized water and anhydrous ethanol were used to wash the precipitates. Finally, desiccation at 60 °C and calcination at 550 °C for 4 h in static air were conducted.

An impregnation method was used to synthesize NbO_x/CeO_2 catalysts with nanosized CeO_2 as support. The nominal loading of niobia (calculated as Nb_2O_5) was 20 wt %. First, the CeO_2 was impregnated in a niobium oxalate solution. After stirring, a rotary evaporator was used to eliminate the excess water. Finally, the samples were dried overnight, followed by calcining at 500 °C in static air for 3 h.

2.2. Activity Testing. The tests were conducted with 0.6 mL of the catalysts (40−60 mesh) at atmospheric pressure in a fixed-bed quartz flow reactor. O_2 (5 vol %), NH_3 (500 ppm), and NO (500 ppm) were in the feed gas, and the gas hourly space velocity (GHSV) was 50 000 h^{-1}. A Fourier transform infrared (FTIR) gas analyzer (Thermo Fisher IGS) was used to analyzed the exit gases (NH_3, NO_2, NO, and N_2O).

2.3. Characterization. A transmission electron microscope (TEM; FEI Tecnai G2 F30) with acceleration voltage of 100 kV was applied to collect TEM images.

X-ray diffraction (XRD) measurements of the samples were conducted at 40 mA and 40 kV using Cu Kα radiation by a PANalytical BV Holland X'Pert Pro XRD diffractometer. The 2θ data from 10° to 80° were recorded with step size of 0.07° at 8°·min^{-1}.

A Quantachrome Autosorb iQ2 automatic adsorption instrument was used to measure the Brunauer−Emmett−Teller (BET) surface area at 77 K. Before N_2 physisorption, the samples were outgassed for 5 h at 300 °C. The pore structure and surface area were determined according to the Barrett−Joyner−Halenda (BJH) method from desorption branches of the isotherms and the BET equation in 0.05−0.30 partial pressure range, respectively.

X-ray photoelectron spectroscopic (XPS) measurements were conducted on a PHI Quantum 2000 scanning ESCA microprobe with a monochromatized microfocused Al X-ray source. C 1s was used as the reference energy (C 1s = 284.6 eV) to calibrate the binding energies.

A Quantachrome ChemStar instrument was applied to perform temperature-programmed reduction with H_2 (H_2-TPR) experiments. The catalysts were pretreated in 100 mL/min Ar flow for 30 min at 400 °C, followed by cooling down to 50 °C and purging with an Ar flow for 30 min. Finally, the reduction temperature was raised linearly to 1000 °C in 5 vol % H_2/Ar (100 mL/min) at a rate of 10 °C/min.

2.4. Diffuse Reflectance Infrared Fourier Transform Spectroscopic Studies. Diffuse reflectance infrared Fourier transform spectroscopic (DRIFTS) measurements of NO_x/NH_3 adsorption on ceria-based samples were conducted on a Thermo Fisher Nicolet iS50 FTIR spectrometer. The sample was cooled to 225 °C after being pretreated for 30 min in 20 vol % O_2/N_2 at 300 °C, followed by purging with N_2 for background collection. The reaction conditions were controlled as follows: 500 ppm NO + 5 vol % O_2/N_2, or 500 ppm NH_3/N_2, 300 mL/min total flow rate. All spectra were recorded by accumulating 100 scans with a resolution of 4 cm^{-1}.

3. RESULTS AND DISCUSSION

3.1. Morphology and Structural Properties. The morphology of the CeO_2 nanomaterials was characterized by TEM. Figure 1 shows that three different morphologies of CeO_2 nanomaterials, including nanocubes (NC), nanoparticles (NP), and nanorods (NR), had all been successfully synthesized. After the deposition of Nb, the three CeO_2 nanomaterials mostly retained their original morphologies, and no structural features of Nb compounds could be observed. This indicates that Nb was highly dispersed on these samples.

Table 1 shows the textural parameters of Nb/CeO_2 NR, NP, and NC samples. Among the three catalysts, the Nb/CeO_2 NP sample presented the smallest average pore diameter and the largest surface area, which are potentially favorable for the SCR reaction, followed by Nb/CeO_2 NR. Nb/CeO_2 NC presented the largest pore diameter and the smallest specific surface area.

Table 1. Textural Features of Nb/CeO_2 Samples

catalyst	pore volume (cm^3/g)	pore diameter (nm)	specific surface area (m^2/g)
Nb/CeO_2 NC	0.16	17.2	36.3
Nb/CeO_2 NP	0.22	9.40	92.1
Nb/CeO_2 NR	0.23	12.0	75.3

DOI: 10.1021/acs.iecr.8b02553
Ind. Eng. Chem. Res. 2018, 57, 12736−12741

Powder XRD results of Nb/CeO_2 samples are exhibited in Figure 2. These Nb/CeO_2 materials could be indexed to a pure

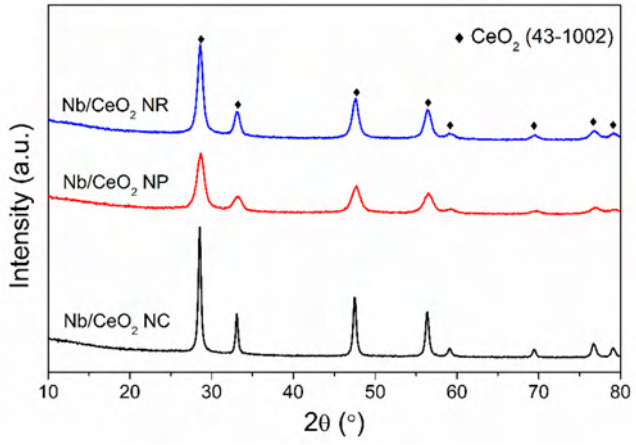

Figure 2. Powder XRD patterns of Nb/CeO_2 catalysts.

fluorite cubic CeO_2 structure (JCPDS 43-1002). Nb/CeO_2 NP presented the lowest crystallinity, while Nb/CeO_2 NC showed the highest crystallinity. The large specific surface area could be related to the low crystallinity. No diffraction peaks from niobium species were observed in these samples, demonstrating the high dispersion of Nb.

3.2. Redox Properties. XPS can be used to analyze the surface chemistry on Nb/CeO_2 samples. Figure 3A shows the spectra of Ce 3d on Nb/CeO_2 catalysts, which were fitted by eight components according to the literature.[29−32] The v′ and u′ bands represented the $3d^{10}$ $4f^1$ initial electronic state corresponding to Ce^{3+}, while the $3d^{10}$ $4f^0$ state of Ce^{4+} was labeled as v, u, v″, u″, v‴, and u‴. Figure 3A also lists the relative surface concentration ratio of Ce^{3+}, which was determined from the corresponding peak areas. The surface Ce^{3+} ratio on Nb/CeO_2 NP was 19.88%, slightly higher than that on Nb/CeO_2 NC and NR. More Ce^{3+} contributed to form oxygen vacancies, favorable for forming chemisorbed oxygen species by adsorbing oxygen on the catalyst surface.

Figure 3B presents the Nb 3d spectra. According to the literature,[27,33,34] the peaks centered at 209.5 and 206.7 eV, representing Nb $3d_{3/2}$ and Nb $3d_{5/2}$ with a spin−orbit splitting of 2.8 eV, were ascribed to Nb^{5+} species. The three Nb/CeO_2 samples showed the same Nb valence state.

The O 1s spectra obtained on Nb/CeO_2 samples are exhibited in Figure 3C. The peaks at 529.5−530.0 and 531.7−532.7 eV could be attributed to lattice oxygen O^{2-} (denoted as O_β) and surface-adsorbed oxygen (denoted as O_α), respectively.[24,27] In oxidation reactions, O_α, with higher mobility, is more reactive than O_β.[35−37] Therefore, a high O_α ratio could favor the oxidation of NO to NO_2 and then contribute to the fast SCR reaction. The relative surface concentration ratios of O_α/O_{all} on Nb/CeO_2 catalysts were determined from the corresponding peak areas and are listed in Figure 3C. The O_α/O_{all} ratios of Nb/CeO_2 NP were the highest among the three catalysts, demonstrating the presence of the most abundant surface oxygen, consistent with the Ce^{3+}/Ce_{all} ratios presented in Figure 3A.

Figure 4 exhibits the H_2-TPR results of ceria-based catalysts. For the CeO_2 samples, two main peaks at 400−600 and 700−

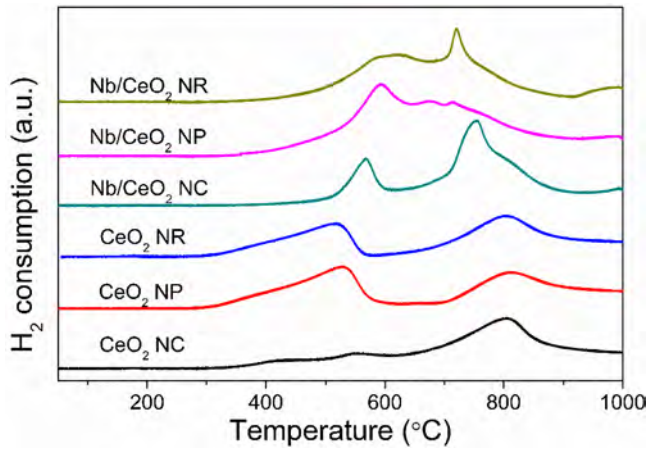

Figure 4. H_2-TPR results of CeO_2 samples and Nb/CeO_2 catalysts.

800 °C were observed, ascribed to the reduction of surface Ce^{4+} to Ce^{3+} and of bulk Ce^{4+} to Ce^{3+}, respectively.[38,39] CeO_2 NC showed a much weaker reduction peak than CeO_2 NR and NP at low temperature, indicating weaker redox capability. The reduction peaks at low temperature shifted to higher temperature after the deposition of Nb. The amount of H_2 consumption for Nb/CeO_2 NP below 650 °C was larger than

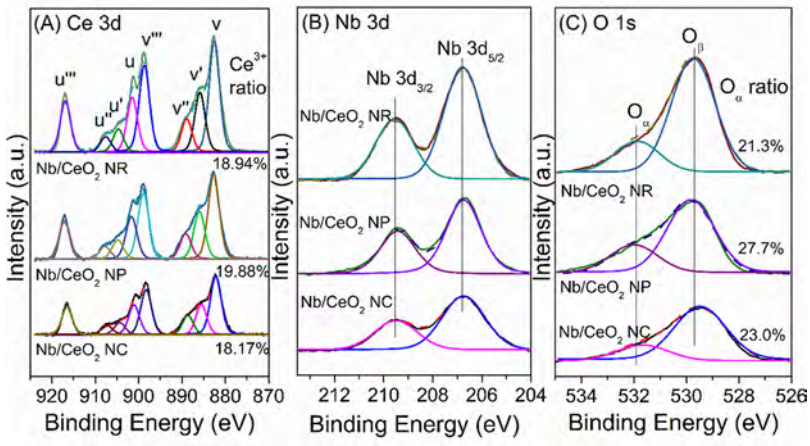

Figure 3. XPS results of (A) Ce 3d, (B) Nb 3d, and (C) O 1s of Nb/CeO_2 catalysts.

DOI: 10.1021/acs.iecr.8b02553
Ind. Eng. Chem. Res. 2018, 57, 12736−12741

that of Nb/CeO_2 NR and NC. Among the three catalysts, the onset temperature of H_2 reduction over Nb/CeO_2 NP was the lowest, while that over Nb/CeO_2 NC was the highest. In general, the NH_3-SCR reaction mainly takes place below 650 °C. Therefore, compared with Nb/CeO_2 NR and NC, the strong redox capability of Nb/CeO_2 NP at low temperature could enhance NH_3-SCR performance.

In order to study the surface acidity of Nb/CeO_2 samples, NH_3-TPD measurements were carried out (Figure 5). Nb/

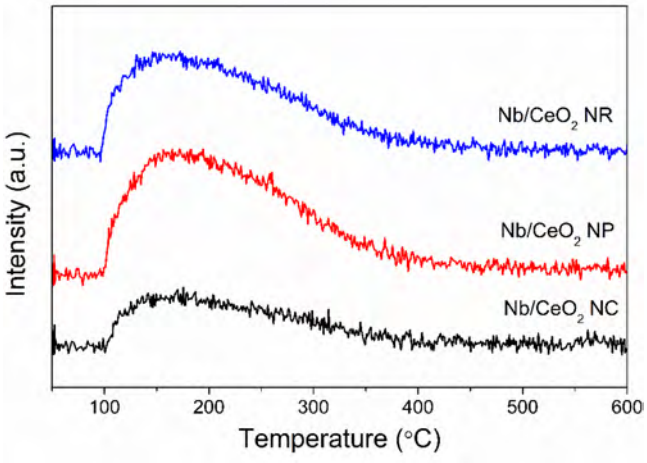

Figure 5. NH_3-TPD results of Nb/CeO_2 samples.

CeO_2 NC desorbed a small amount of NH_3. The area of NH_3 desorption peaks of the three catalysts decreased in the following sequence: Nb/CeO_2 NP > NR > NC. The Nb/CeO_2 NP catalyst showed the most acid sites.

3.3. Diffuse Reflectance Infrared Fourier Transform Spectroscopy. DRIFTS was performed at 225 °C to study NH_3/NO_x adsorption on the ceria-based samples. Figure 6A

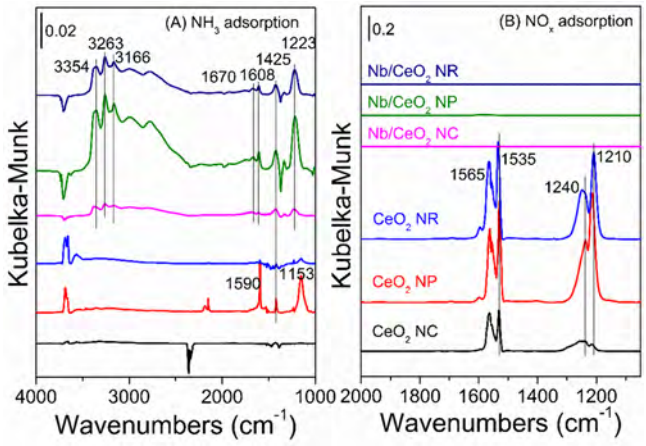

Figure 6. DRIFT spectra of (A) NH_3 adsorption and (B) NO + O_2 adsorption on CeO_2 samples and Nb/CeO_2 catalysts at 225 °C.

exhibits the results of ammonia adsorption. Several adsorbed ammonia species were detected on the samples after NH_3 adsorption. The peaks at 1425 and 1670 cm^{-1} were attributed to the asymmetric and symmetric bending vibrations of NH_4^+ on Brønsted acid sites, while the peaks at 1608 (1590) and 1223 (1153) cm^{-1} were assigned to asymmetric and symmetric bending vibrations of NH_3 coordinated on Lewis acid sites.[40−43] The peaks attributed to the NH stretching vibration were observed at 3354, 3263, and 3166 cm^{-1}.[30,40] There were almost no adsorbed NH_3 species on CeO_2 NR and NC. The deposition of Nb increased the amount of acid sites on the samples, in accordance with previous reports.[24,25] The Nb/CeO_2 NP catalyst presented the largest amount of adsorbed NH_3 species, illustrating that it possessed the most abundant acid sites, consistent with the results of NH_3-TPD.

DRIFTS of NO_x adsorption on ceria-based samples at 225 °C was also conducted (Figure 6B). The surface was covered with nitrate species after the CeO_2 samples were exposed to NO + O_2, including bidentate nitrate (1565 and 1240 cm^{-1}), bridging nitrate (1210 cm^{-1}), and monodentate nitrate (1535 cm^{-1}).[44,45] However, after the deposition of Nb, no adsorbed NO_x species were detected. According to the literature,[46] the introduction of niobia could enhance the acidity and lower the intensity of the nitrate-related bands. The strong acidity could strongly hinder the formation of nitrate species.[36,47,48] Therefore, the fact that no NO_x species were adsorbed on the Nb/CeO_2 samples might be due to inhibition by the enhancement of acidity.

3.4. Catalytic Performance and Discussion. The catalytic activity at various temperatures for SCR over the Nb/CeO_2 catalysts is exhibited in Figure 7. We can see that the

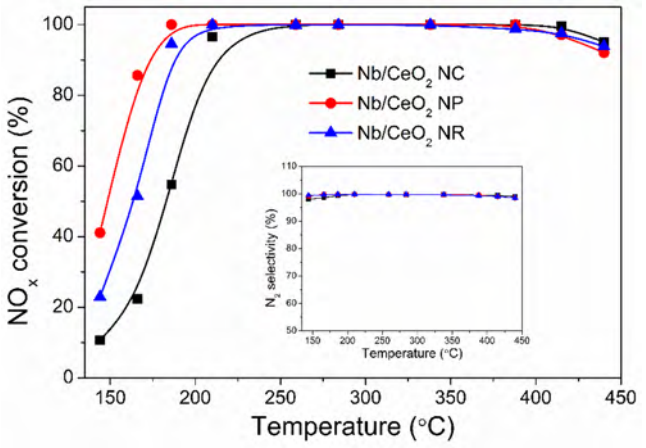

Figure 7. SCR activity over Nb/CeO_2 catalysts.

CeO_2 morphologies could indeed influence the SCR performance of Nb/CeO_2 catalysts. The NO_x conversion decreased in the following sequence at temperatures below 250 °C: Nb/CeO_2 NP > NR > NC. The Nb/CeO_2 NP catalyst presented the highest SCR activity, and the NO_x conversion at 180−440 °C was nearly 100%. The N_2 selectivities over the three catalysts were almost 100% over the whole temperature range investigated. Nb/CeO_2 NP also showed strong H_2O and SO_2 resistance (Figure 8). The existence of H_2O and SO_2 did not decrease the activity of Nb/CeO_2 NP.

Even though all Nb/CeO_2 catalysts had the same Nb loadings, their NH_3-SCR catalytic performance depended on the morphology of CeO_2. XRD and BET results show that Nb/CeO_2 NP synthesized from CeO_2 nanoparticles presented the lowest crystallinity and the largest specific surface area, followed by Nb/CeO_2 NR, and Nb/CeO_2 NC exhibited the highest crystallinity and the smallest specific surface area. Lower crystallinity and larger specific surface area signify better dispersion of Nb and more defects on the surface. Therefore, Nb/CeO_2 NP had more surface Ce^{3+} and surface-active

DOI: 10.1021/acs.iecr.8b02553
Ind. Eng. Chem. Res. 2018, 57, 12736−12741

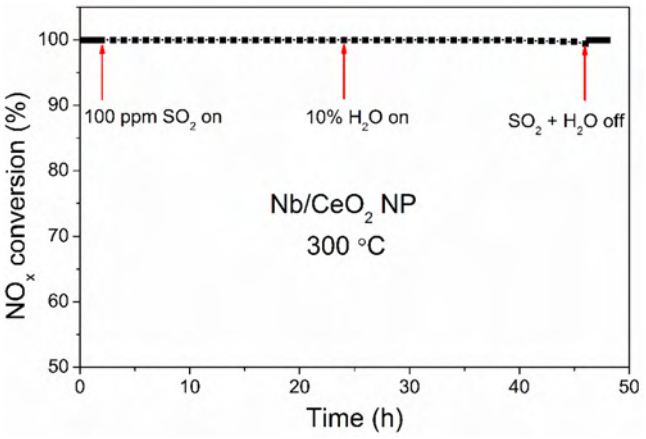

Figure 8. Influence of SO_2 and H_2O on SCR activity of Nb/CeO_2 NP.

oxygen. Nb/CeO_2 NP presented strong redox capability at low temperature. Meanwhile, from the DRIFTS results we can see that more acid sites were obtained on Nb/CeO_2 NP, resulting from better dispersion of Nb and larger specific surface area. This could facilitate the adsorption and activation of ammonia. Therefore, excellent catalytic activity was obtained with Nb/CeO_2 NP.

4. CONCLUSIONS

A systematic investigation was conducted on the influence of morphology on Nb/CeO_2 catalysts for selective catalytic reduction of NO_x with NH_3. Among nanocubes, nanoparticles, and nanorods, the Nb/CeO_2 NP catalyst derived from CeO_2 nanoparticles exhibited the best catalytic performance, and almost 100% NO_x conversion was obtained at 180−440 °C. The lower crystallinity and larger specific surface area of Nb/CeO_2 NP implied the presence of better dispersion of Nb species and more defects on the surface. Consequently, Nb/CeO_2 NP presents more surface oxygen, more acid sites and stronger redox capability. Due to these factors, excellent NH_3-SCR activity was obtained with Nb/CeO_2 NP.

AUTHOR INFORMATION

Corresponding Author

*Fax: +86 592 6190990. Telephone: +86 592 6190990. E-mail: honghe@rcees.ac.cn or hhe@iue.ac.cn.

ORCID

Zhihua Lian: 0000-0002-7413-180X

Notes

The authors declare no competing financial interest.

ACKNOWLEDGMENTS

The study was financially supported by National Key R&D Program of China (2016YFC0205301), the National Natural Science Foundation of China (21607149), Key Project of National Natural Science Foundation (21637005), Natural Science Foundation of Fujian Province, China (2016J05142), and Key Program of the Chinese Academy of Sciences (ZDRW-ZS-2017-6-2-3).

REFERENCES

(1) Qi, G. S.; Yang, R. T.; Chang, R. MnO_x-CeO_2 mixed oxides prepared by co-precipitation for selective catalytic reduction of NO with NH_3 at low temperatures. *Appl. Catal., B* **2004**, *51*, 93.

(2) Bosch, H.; Janssen, F. Formation and control of nitrogen oxides. *Catal. Today* **1988**, *2*, 369.

(3) Busca, G.; Lietti, L.; Ramis, G.; Berti, F. Chemical and mechanistic aspects of the selective catalytic reduction of NO_x by ammonia over oxide catalysts: A review. *Appl. Catal., B* **1998**, *18*, 1.

(4) Roy, S.; Hegde, M. S.; Madras, G. Catalysis for NO_x abatement. *Appl. Energy* **2009**, *86*, 2283.

(5) Kristensen, S. B.; Kunov-Kruse, A. J.; Riisager, A.; Rasmussen, S. B.; Fehrmann, R. High performance vanadia−anatase nanoparticle catalysts for the Selective Catalytic Reduction of NO by ammonia. *J. Catal.* **2011**, *284*, 60.

(6) Forzatti, P. Present status and perspectives in de-NO_x SCR catalysis. *Appl. Catal., A* **2001**, *222*, 221.

(7) Smirniotis, P. G.; Pena, D. A.; Uphade, B. S. Low-temperature selective catalytic reduction (SCR) of NO with NH_3 by using Mn, Cr, and Cu oxides supported on Hombikat TiO_2. *Angew. Chem., Int. Ed.* **2001**, *40*, 2479.

(8) Putluru, S. S. R.; Schill, L.; Jensen, A. D.; Siret, B.; Tabaries, F.; Fehrmann, R. Mn/TiO_2 and $Mn-Fe/TiO_2$ catalysts synthesized by deposition precipitation-promising for selective catalytic reduction of NO with NH_3 at low temperatures. *Appl. Catal., B* **2015**, *165*, 628.

(9) Lian, Z.; Liu, F.; He, H. Effect of preparation methods on the activity of VO_x/CeO_2 catalysts for the selective catalytic reduction of NO_x with NH_3. *Catal. Sci. Technol.* **2015**, *5*, 389.

(10) Xu, W.; Yu, Y.; Zhang, C.; He, H. Selective catalytic reduction of NO by NH_3 over a Ce/TiO_2 catalyst. *Catal. Commun.* **2008**, *9*, 1453.

(11) Shan, W.; Liu, F.; He, H.; Shi, X.; Zhang, C. An environmentally-benign CeO_2-TiO_2 catalyst for the selective catalytic reduction of NO_x with NH_3 in simulated diesel exhaust. *Catal. Today* **2012**, *184*, 160.

(12) Zhang, L.; Sun, J.; Xiong, Y.; Zeng, X.; Tang, C.; Dong, L. Catalytic performance of highly dispersed WO_3 loaded on CeO_2 in the selective catalytic reduction of NO by NH_3. *Chin. J. Catal.* **2017**, *38*, 1749.

(13) Chen, L.; Li, J.; Ablikim, W.; Wang, J.; Chang, H.; Ma, L.; Xu, J.; Ge, M.; Arandiyan, H. CeO_2-WO_3 mixed oxides for the selective catalytic reduction of NO_x by NH_3 over a wide temperature range. *Catal. Lett.* **2011**, *141*, 1859.

(14) Song, Z.; Zhang, Q.; Ma, Y.; Liu, Q.; Ning, P.; Liu, X.; Wang, J.; Zhao, B.; Huang, J.; Huang, Z. Mechanism-dependent on the different CeO_2 supports of phosphotungstic acid modification CeO_2 catalysts for the selective catalytic reduction of NO with NH_3. *J. Taiwan Inst. Chem. Eng.* **2017**, *71*, 277.

(15) Weng, X.; Dai, X.; Zeng, Q.; Liu, Y.; Wu, Z. DRIFT studies on promotion mechanism of $H_3PW_{12}O_{40}$ in selective catalytic reduction of NO with NH_3. *J. Colloid Interface Sci.* **2016**, *461*, 9.

(16) Wang, L.; Wang, Y.; Zhang, Y.; Yu, Y.; He, H.; Qin, X.; Wang, B. Shape dependence of nanoceria on complete catalytic oxidation of o-xylene. *Catal. Sci. Technol.* **2016**, *6*, 4840.

(17) Zhang, Y.; Yu, Y.; He, H. Oxygen vacancies on nanosized ceria govern the NO_x storage capacity of NSR catalysts. *Catal. Sci. Technol.* **2016**, *6*, 3950.

(18) Shi, Q.; Li, Y.; Zhou, Y.; Miao, S.; Ta, N.; Zhan, E.; Liu, J.; Shen, W. The shape effect of TiO_2 in VO_x/TiO_2 catalysts for selective reduction of NO by NH_3. *J. Mater. Chem. A* **2015**, *3*, 14409.

(19) Zhao, X.; Huang, L.; Namuangruk, S.; Hu, H.; Hu, X.; Shi, L.; Zhang, D. Morphology-dependent performance of $Zr-CeVO_4/TiO_2$ for selective catalytic reduction of NO with NH_3. *Catal. Sci. Technol.* **2016**, *6*, 5543.

(20) Liu, J.; Meeprasert, J.; Namuangruk, S.; Zha, K.; Li, H.; Huang, L.; Maitarad, P.; Shi, L.; Zhang, D. Facet−Activity Relationship of TiO_2 in Fe_2O_3/TiO_2 Nanocatalysts for Selective Catalytic Reduction of NO with NH_3: In Situ DRIFTs and DFT Studies. *J. Phys. Chem. C* **2017**, *121*, 4970.

(21) Song, L.; Zhang, R.; Zang, S.; He, H.; Su, Y.; Qiu, W.; Sun, X. Activity of Selective Catalytic Reduction of NO over V_2O_5/TiO_2 Catalysts Preferentially Exposed Anatase {001} and {101} Facets. *Catal. Lett.* **2017**, *147*, 934.

DOI: 10.1021/acs.iecr.8b02553
Ind. Eng. Chem. Res. 2018, 57, 12736−12741

(22) Han, J.; Meeprasert, J.; Maitarad, P.; Nammuangruk, S.; Shi, L.; Zhang, D. Investigation of the Facet-Dependent Catalytic Performance of Fe_2O_3/CeO_2 for the Selective Catalytic Reduction of NO with NH_3. *J. Phys. Chem. C* **2016**, *120*, 1523.
(23) Tanabe, K. Catalytic application of niobium compounds. *Catal. Today* **2003**, *78*, 65.
(24) Lian, Z.; Liu, F.; He, H.; Shi, X.; Mo, J.; Wu, Z. Manganese–niobium mixed oxide catalyst for the selective catalytic reduction of NO_x with NH_3 at low temperatures. *Chem. Eng. J.* **2014**, *250*, 390.
(25) Lian, Z.; Liu, F.; He, H.; Liu, K. Nb-doped VO_x/CeO_2 catalyst for NH_3-SCR of NO_x at low temperatures. *RSC Adv.* **2015**, *5*, 37675.
(26) Ding, S.; Liu, F.; Shi, X.; He, H. Promotional effect of Nb additive on the activity and hydrothermal stability for the selective catalytic reduction of NO_x with NH_3 over $CeZrO_x$ catalyst. *Appl. Catal., B* **2016**, *180*, 766.
(27) Zhao, B.; Ran, R.; Guo, X.; Cao, L.; Xu, T.; Chen, Z.; Wu, X.; Si, Z.; Weng, D. Nb-modified Mn/Ce/Ti catalyst for the selective catalytic reduction of NO with NH_3 at low temperature. *Appl. Catal., A* **2017**, *545*, 64.
(28) Casapu, M.; Krocher, O.; Mehring, M.; Nachtegaal, M.; Borca, C.; Harfouche, M.; Grolimund, D. Characterization of Nb-containing MnO_x-CeO_2 catalyst for low-temperature selective catalytic reduction of NO with NH_3. *J. Phys. Chem. C* **2010**, *114*, 9791.
(29) Liu, J.; Du, Y.; Liu, J.; Zhao, Z.; Cheng, K.; Chen, Y.; Wei, Y.; Song, W.; Zhang, X. Design of MoFe/Beta@CeO_2 catalysts with a core-shell structure and their catalytic performances for the selective catalytic reduction of NO with NH_3. *Appl. Catal., B* **2017**, *203*, 704.
(30) Gao, G.; Shi, J.-W.; Liu, C.; Gao, C.; Fan, Z.; Niu, C. Mn/CeO_2 catalysts for SCR of NO_x with NH_3: comparative study on the effect of supports on low-temperature catalytic activity. *Appl. Surf. Sci.* **2017**, *411*, 338.
(31) Chen, T.; Lin, H.; Cao, Q.; Huang, Z. Solution combustion synthesis of $Ti_{0.75}Ce_{0.15}Cu_{0.05}W_{0.05}O_{2\text{-delta}}$ for low temperature selective catalytic reduction of NO. *RSC Adv.* **2014**, *4*, 63909.
(32) Wang, X.; Zhang, K.; Zhao, W.; Zhang, Y.; Lan, Z.; Zhang, T.; Xiao, Y.; Zhang, Y.; Chang, H.; Jiang, L. Effect of Ceria Precursor on the Physicochemical and Catalytic Properties of Mn-W/CeO_2 Nanocatalysts for NH_3 SCR at Low Temperature. *Ind. Eng. Chem. Res.* **2017**, *56*, 14980.
(33) Ma, Z.; Wu, X.; Si, Z.; Weng, D.; Ma, J.; Xu, T. Impacts of niobia loading on active sites and surface acidity in NbO_x/CeO_2-ZrO_2 NH_3-SCR catalysts. *Appl. Catal., B* **2015**, *179*, 380.
(34) Wang, Y.; Smarsly, B. M.; Djerdj, I. Niobium Doped TiO_2 with Mesoporosity and Its Application for Lithium Insertion. *Chem. Mater.* **2010**, *22*, 6624.
(35) Yan, L.; Liu, Y.; Zha, K.; Li, H.; Shi, L.; Zhang, D. Scale activity relationship of MnO_x-FeO_y nanocage catalysts derived from Prussian blue analogues for low-temperature NO reduction: experimental and DFT studies. *ACS Appl. Mater. Interfaces* **2017**, *9*, 2581.
(36) Maqbool, M. S.; Pullur, A. K.; Ha, H. P. Novel sulfation effect on low-temperature activity enhancement of CeO_2-added Sb-V_2O_5/TiO_2 catalyst for NH_3-. *Appl. Catal., B* **2014**, *152-153*, 28.
(37) Gao, X.; Li, L.; Song, L.; Lu, T.; Zhao, J.; Liu, Z. Highly dispersed MnOx nanoparticles supported on three-dimensionally ordered macroporous carbon: a novel nanocomposite for catalytic reduction of NOx with NH3 at low temperature. *RSC Adv.* **2015**, *5*, 29577.
(38) Zhang, T.; Qiu, F.; Chang, H.; Peng, Y.; Li, J. Novel W-modified $SnMnCeO_x$ catalyst for the selective catalytic reduction of NO_x with NH_3. *Catal. Commun.* **2017**, *100*, 117.
(39) Zhao, K.; Han, W.; Lu, G.; Lu, J.; Tang, Z.; Zhen, X. Promotion of redox and stability features of doped Ce-W-Ti for NH_3-SCR reaction over a wide temperature range. *Appl. Surf. Sci.* **2016**, *379*, 316.
(40) Xu, H.; Feng, X.; Liu, S.; Wang, Y.; Sun, M.; Wang, J.; Chen, Y. Promotional effects of Titanium additive on the surface properties, active sites and catalytic activity of W/$CeZrO_x$ monolithic catalyst for the selective catalytic reduction of NO_x with NH_3. *Appl. Surf. Sci.* **2017**, *419*, 697.
(41) Lee, K. J.; Kumar, P. A.; Maqbool, M. S.; Rao, K. N.; Song, K. H.; Ha, H. P. Ceria added Sb-V_2O_5/TiO_2 catalysts for low temperature NH_3 SCR: Physico-chemical properties and catalytic activity. *Appl. Catal., B* **2013**, *142-143*, 705.
(42) Zhan, S.; Zhu, D.; Qiu, M.; Yu, H.; Li, Y. Highly efficient removal of NO with ordered mesoporous manganese oxide at low temperature. *RSC Adv.* **2015**, *5*, 29353.
(43) Sun, J.; Lu, Y.; Zhang, L.; Ge, C.; Tang, C.; Wan, H.; Dong, L. Comparative Study of Different Doped Metal Cations on the Reduction, Acidity, and Activity of $Fe_9M_1O_x$ (M = Ti^{4+}, $Ce^{4+/3+}$, Al^{3+}) Catalysts for NH3-SCR Reaction. *Ind. Eng. Chem. Res.* **2017**, *56*, 12101.
(44) Yao, X.; Kong, T.; Chen, L.; Ding, S.; Yang, F.; Dong, L. Enhanced low-temperature NH_3-SCR performance of MnO_x/CeO_2 catalysts by optimal solvent effect. *Appl. Surf. Sci.* **2017**, *420*, 407.
(45) Yang, N. Z.; Guo, R. T.; Pan, W. G.; Chen, Q. L.; Wang, Q. S.; Lu, C. Z.; Wang, S. X. The deactivation mechanism of Cl on Ce/TiO_2 catalyst for selective catalytic reduction of NO with NH_3. *Appl. Surf. Sci.* **2016**, *378*, 513.
(46) Ma, Z.; Wu, X.; Harelind, H.; Weng, D.; Wang, B.; Si, Z. NH_3-SCR reaction mechanisms of $NbO_x/Ce_{0.75}Zr_{0.25}O_2$ catalyst: DRIFTS and kinetics studies. *J. Mol. Catal. A: Chem.* **2016**, *423*, 172.
(47) Liu, F.; Asakura, K.; He, H.; Shan, W.; Shi, X.; Zhang, C. Influence of sulfation on iron titanate catalyst for the selective catalytic reduction of NO_x with NH_3. *Appl. Catal., B* **2011**, *103*, 369.
(48) Ding, S.; Liu, F.; Shi, X.; Liu, K.; Lian, Z.; Xie, L.; He, H. Significant Promotion Effect of Mo Additive on a Novel Ce-Zr Mixed Oxide Catalyst for the Selective Catalytic Reduction of NOx with NH_3. *ACS Appl. Mater. Interfaces* **2015**, *7*, 9497.

DOI: 10.1021/acs.iecr.8b02553
Ind. Eng. Chem. Res. 2018, 57, 12736–12741